

Distribution of Observed C–H Bond Lengths in Neutron Crystal Structures and Temperature Dependence of the Mean Values

BY T. STEINER AND W. SAENGER

Institut für Kristallographie, Freie Universität Berlin, Takustrasse 6, W-1000 Berlin 33, Germany

(Received 24 July 1992; accepted 30 September 1992)

Abstract

An analysis is given of C–H bond lengths and their apparent shortening by thermal vibrations in neutron crystal structures. D atoms were excluded. Mean bond lengths and the spread of observed values were compiled for six different chemical connectivities in three temperature ranges (room temperature, $80 \leq T < 125$ and $T < 30$ K). At low temperatures ($T < 30$ K), the mean values agree very well with spectroscopic data. Owing to thermal vibrations, the average observed C–H bond length in methyl groups at room temperature (1.057 Å) is shortened by 0.03 Å compared with that at $T < 30$ K (1.088 Å). The shortening reduces only slowly upon cooling and is still significant at temperatures around 100 K. For the other connectivities, in which the C–H orientations are more rigidly confined, the average shortening at room temperature is 0.01 to 0.02 Å, and at $T \sim 100$ K the mean observed bond lengths have already (or almost) reached the spectroscopic values. The distributions of the observed bond lengths are asymmetric with the maxima at distances greater than the average. The positions of the maxima are less affected by temperature changes than the average values, implying that at room temperature many bond lengths are only slightly affected by thermal motions.

Introduction

The appropriate crystallographic technique to determine X–H bond lengths (d_{XH}) is neutron diffraction. Because of the apparent bond shortening caused by charge-density distortions [on the average 0.1 Å for C–H (Allen, 1986)], X-ray data are generally unsuitable in this context. In the following, we concentrate on C–H bond lengths, d_{CH} , for which the largest body of neutron diffraction data is available. For a given chemical type of C–H, neutron-determined d_{CH} show a significant temperature dependence and, at any given temperature, the values of d_{CH} vary considerably. These variations are (apart from experimental uncertainty) primarily due to thermal vibrations of the H atom. In contrast to O–H and N–H, the influence of hydrogen-bonding effects on d_{CH} is only marginal (Steiner & Saenger, 1992) and will not be considered here any further.

In crystals, neutron diffraction observes the time and lattice average of vibrating atomic nuclei. These represent three-dimensional probability density functions (p.d.f.s), which in most cases are Gaussian-like with more or less pronounced deviations from the ideal shape (Johnson & Levy, 1974). Deviations from a Gaussian shape are caused, for example, by curvilinear motion of librating atoms and bond-stretching vibrations in anharmonic potentials. In conventional anisotropic refinement, the Gaussian-like p.d.f.s are approximated by ideal Gaussian functions (six thermal parameters), leading to systematic errors if a p.d.f. deviates significantly from the Gaussian function. This is actually observed for H atoms, which generally vibrate vigorously owing to their small weight and their terminal position. In principle, one can resort to more sophisticated models of the p.d.f. at the price of refining more parameters (Johnson & Levy, 1974), but in practice this is performed only in exceptional cases (for examples, see Kuhs, 1983).

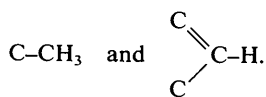
Most published neutron crystal structures are based on conventional refinement, which leads to systematic shifts of observed H-atom positions along the X–H bond in the direction of X, *i.e.* to reductions of the observed bond length d_{XH} . Methods for (rough) correction of d_{XH} based on the refined anisotropic thermal parameters of X and H have been proposed: librations perpendicular to the X–H bond lead to an apparent reduction of d_{XH} that can be estimated by the well known ‘riding-motion’ model (Busing & Levy, 1964), whereas anharmonic vibrations along the X–H bond lengthen d_{XH} ; a corresponding correction was suggested by Weber, Craven & McMullan (1983) that is based on Morse potential functions obtained from the gas phase. Application of the riding-motion model alone leads to overcorrection (Jeffrey, Ruble, McMullan, DeFrees & Pople, 1981; Srinivasan & Jagannathan, 1982), but application of both corrections produces bond lengths that are consistent with spectroscopic data (Craven & Swaminathan, 1984). At low temperatures, both effects almost cancel, whereas at room temperature a net shortening is observed. In addition, vibrations of the molecules as a whole (Schomaker & Trueblood, 1968) or of molecular segments (Dunitz & White, 1973) have to be considered.

In crystal-structure publications, coordinates of the observed (*i.e.* uncorrected) atomic position are given. In the literature, we find a lack of empirical d_{CH} data compilations: in bond-length tabulations, the temperature dependence of observed d_{XH} is usually neglected and only room-temperature values, or even average values of d_{XH} measured at different temperatures, are given. In this study, we present a survey of observed C-H bond lengths for six chemical connectivities of C, the statistical distribution of the observed d_{CH} and the temperature dependence of their mean values. It is primarily addressed to experimentalists and users of crystallographic databases who require statistically relevant reference data to see whether observed C-H bonds fall into the acceptable ranges of d_{CH} or not. This study is purely empirical; it does not comment on the theoretical works mentioned above.

Data analysis

The neutron diffraction subset of the Cambridge Structural Database (CSD) (Allen *et al.*, 1979), July 1991 release, was combined with three recent neutron crystal structures that are rich in well refined C-H bonds: cholesteryl acetate at $T=20$ K (Weber, Craven, Sawzik & McMullan, 1991) and β -cyclodextrin-ethanol octahydrate at $T=15$ and 295 K (Steiner, Mason & Saenger, 1990, 1991). For a characterization of the neutron subset of the CSD, see Allen (1986).

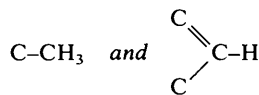
As a quality criterion, only the R value was used. To find a justification for a certain cutoff in R , an initial analysis of C-H bond lengths was performed for the two most frequent connectivities at room temperature,



The number of published C-H bonds and the corresponding mean lengths $\langle d_{\text{CH}} \rangle$ at room temperature are listed for five R ranges in Table 1. The structures with $R \geq 0.10$ have suspiciously shorter $\langle d_{\text{CH}} \rangle$ values than the better refined ones; as their number is relatively small, they can be excluded without significant loss in data quantity. For $0.08 \leq R < 0.10$, $\langle d_{\text{CH}} \rangle$ is slightly shorter than for $R < 0.08$. As the difference is small, however, and over 25% of the available room-temperature data fall into this range, we use the quality criterion $R < 0.10$ throughout this study.

Deuteration must have a distinct effect on the hydrogen vibration behaviour. The number of neutron structures describing molecules with C-D groups, however, is still too small for a comparison of the temperature dependence of average C-H and C-D bond lengths with good statistical significance.

Table 1. R dependence of mean observed C-H bond lengths (D atoms excluded) at room temperature in



n_{struct} : number of neutron crystal structures. n_{CH} : number of symmetrically independent C-H bonds. $\langle d_{\text{CH}} \rangle$: mean C-H bond length, standard deviation of the mean value (in parentheses) estimated by e.s.d. = $[\sum_i (\langle d_{\text{CH}} \rangle - d_{\text{CH},i})^2 / (n-1)]^{1/2}$. r.m.s. dev.: root-mean-square deviation of d_{CH} from $\langle d_{\text{CH}} \rangle$, calculated by r.m.s. dev. = $[\sum_i (\langle d_{\text{CH}} \rangle - d_{\text{CH},i})^2 / n]^{1/2}$.

R range	n_{struct}	n_{CH}	$\langle d_{\text{CH}} \rangle$	R.m.s. dev.
C-CH₃				
$0.10 \leq R$	3	18	1.017 (9)	0.04
$0.08 \leq R < 0.10$	13	99	1.054 (6)	0.06
$0.06 \leq R < 0.08$	12	87	1.060 (4)	0.04
$0.04 \leq R < 0.06$	12	111	1.052 (5)	0.05
$R < 0.04$	10	93	1.063 (6)	0.06
C=C-H				
$0.10 \leq R$	6	41	1.042 (12)	0.08
$0.08 \leq R < 0.10$	22	143	1.066 (4)	0.04
$0.06 \leq R < 0.08$	16	105	1.077 (4)	0.04
$0.04 \leq R < 0.06$	28	182	1.074 (3)	0.03
$R < 0.04$	16	74	1.079 (2)	0.02

Such a (certainly interesting) study must therefore be postponed and C-D bonds were excluded from the present analysis.

Structures with C-H groups constrained in refinement and disordered H and C positions were also excluded. Unusually short or long C-H bonds were only excluded if they were obviously due to typing errors in the CSD or in the original publication. All other C-H bonds were included in the analysis, so that the statistics represent the data 'as published'.

Results

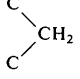
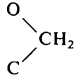
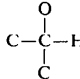
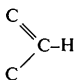
Mean C-H bond lengths in three temperature ranges

In low-temperature neutron diffraction studies, cryostats with liquid nitrogen or liquid helium as coolant are usually employed. In consequence, almost all low-temperature crystal structures fall into the temperature regions $T \sim 100$ and $T < 30$ K. In the first step of the analysis, we therefore considered only data for the three ranges 'room temperature' (RT), $80 \leq T < 125$ K ('medium temperature', MT) and $T < 30$ K ('low temperature', LT).

For these temperature ranges, the numbers of C-H bonds, mean bond lengths $\langle d_{\text{CH}} \rangle$, r.m.s. deviations from $\langle d_{\text{CH}} \rangle$ and examples for corresponding spectroscopic values are shown for several connectivities of C-H in Table 2. Because analyses with small numbers of data tend to show internal inconsistencies, we restricted the study to connectivities for which at least 100 C-H bonds in at least five crystal structures were available in at least one temperature range. Only six

Table 2. Mean uncorrected C–H bond lengths (in Å) for selected connectivities at room temperature at $80 \leq T < 125\text{K}$ and at $T < 30\text{K}$

RT: room temperature; MT: medium temperature ($80 \leq T < 125\text{K}$); LT: low temperature ($T < 30\text{K}$). n_{struct} , n_{CH} , $\langle d_{\text{CH}} \rangle$, r.m.s. dev. defined in Table 1. The spectroscopic data are guide values that are not independent of the experimental method. All spectroscopic data are from Calloman *et al.* (1976).

Connectivity	T	n_{struct}	n_{CH}	$\langle d_{\text{CH}} \rangle$	R.m.s. dev.	Spectroscopy
(1) C–CH ₃	RT	47	390	1.057 (3)	0.053	1.091 (10)*
	MT	12	111	1.082 (2)	0.022	Propane
	LT	19	312	1.088 (1)	0.012	
(2) P–CH ₃	RT	4	51	1.061 (8)	0.054	1.097 (7)*
	MT	2	27	1.089 (2)	0.009	(CH ₃) ₃ P
	LT	8	117	1.089 (1)	0.015	
(3) 	RT	45	208	1.081 (3)	0.048	1.096 (2)*
	MT	11	58	1.093 (3)	0.013	Propane
	LT	8	82	1.100 (1)	0.012	
(4) 	RT	38	146	1.087 (3)	0.020	1.098 (10)*
	MT	9	47	1.095 (1)	0.008	Ethanol
	LT	3	40	1.098 (1)	0.008	
(5) 	RT	41	184	1.095 (1)	0.018	
	MT	6	39	1.105 (2)	0.010	
	LT	2	29	1.105 (2)	0.013	
(6) 	RT	82	504	1.074 (2)	0.034	1.083 (4)†
	MT	34	289	1.084 (1)	0.020	Benzene
	LT	23	345	1.085 (1)	0.010	

* From microwave spectroscopy.

† From infrared spectroscopy.

connectivities satisfied this criterion. For



[connectivity (6)], no distinction was made between localized and delocalized double bonds. This did not lead to inconsistencies and was justified by the narrow r.m.s. deviations found (see below). The total number of data was satisfactory only for connectivities (1) and (6); for the others, it was poor in two temperature ranges for each connectivity. This has to be considered when numeric values are compared.

The low-temperature mean values agree closely with the spectroscopic data. Note that the average bond lengths are shortest for connectivities (1) and (6), and longest for (5). The room-temperature mean values are consistent with the earlier survey by Allen (1986). They are shortened compared with the low-temperature value by, on average, $\sim 0.03\text{Å}$ for methyl groups, almost 0.02Å for methylene groups [connectivity (3)] and $\sim 0.01\text{Å}$ for the other connectivities. Methyl and methylenic C–H bonds are shortened at $T \sim 100\text{K}$ by several thousandths of an Å compared with $T < 30\text{K}$ whereas, for connectivities (5) and (6), the average shortening at $T \sim 100\text{K}$ is within the statistical error.

As expected, the general tendency is that bond shortening is less pronounced the more the C–H orientations are stereochemically rigidly confined. This is also reflected in the r.m.s. deviations from $\langle d_{\text{CH}} \rangle$ at room temperature, which are largest for the methyl groups and smallest for connectivity (5).

Distribution of observed bond lengths at room temperature and at $T < 30\text{K}$

Of the six connectivities in Table 2, the available body of data allows the study of the distribution of observed bond lengths in two temperature ranges with statistical relevance only for (1) and (6). Fig. 1 shows these distributions for room-temperature and low-temperature ($T < 30\text{K}$) data.

For the methyl group bonded to C, the observed room-temperature d_{CH} data show a broad and pronounced asymmetric distribution, with a maximum between 1.075 and 1.080Å and the mean value, $1.057(3)\text{Å}$, shifted by $\sim 0.02\text{Å}$ from the peak maximum (Fig. 1a). A long 'tail' towards the short bond lengths extends to well below 1.0Å . The r.m.s. deviation of 0.053Å is large compared with the typical refinement e.s.d.s of the individual room-temperature structures (0.01 to 0.02Å). The large r.m.s. deviation should not be interpreted as a consequence of poor refinements as the r.m.s. deviations are similar in all the R -value ranges shown in Table 1. At low temperatures ($T < 30\text{K}$), the distribution is narrow with a r.m.s. deviation of 0.012Å (typical refinement e.s.d.: 0.004Å), but it is still asymmetric: it peaks between 1.090 and 1.095Å , with an average, $1.088(1)\text{Å}$, at a slightly shorter value.

For



(Fig. 1b), the general behaviour is similar, but the asymmetry is less pronounced. At room temperature, the distribution of observed d_{CH} peaks between 1.080 and 1.085Å , with an average of $1.074(2)\text{Å}$, shorter than the maximum by $\sim 0.01\text{Å}$, and a r.m.s. deviation of 0.034Å . At low temperatures ($T < 30\text{K}$), the distribution peaks between 1.085 and 1.090Å with an average of $1.085(1)\text{Å}$ and a narrow r.m.s. deviation of 0.010Å .

At room temperature, the distribution of observed d_{CH} is asymmetric even for the stereochemically most rigid connectivity (5): it peaks between 1.100 and 1.105Å with the average at $1.095(1)\text{Å}$ (see Fig. 2). The r.m.s. deviation of 0.018Å , however, is narrower by a factor of 3 compared with the methyl group at room temperature (Table 2).

Despite apparent bond shortening by thermal motions and the large spread of observed bond lengths, the 'true' chemical difference between C–H bond lengths in different connectivities can be clearly

observed not only at low temperature but also at room temperature. This is illustrated in Fig. 2 for connectivities (5) and (6), which at room temperature differ in $\langle d_{\text{CH}} \rangle$ by 0.021 Å and in peak positions by 0.02 Å.

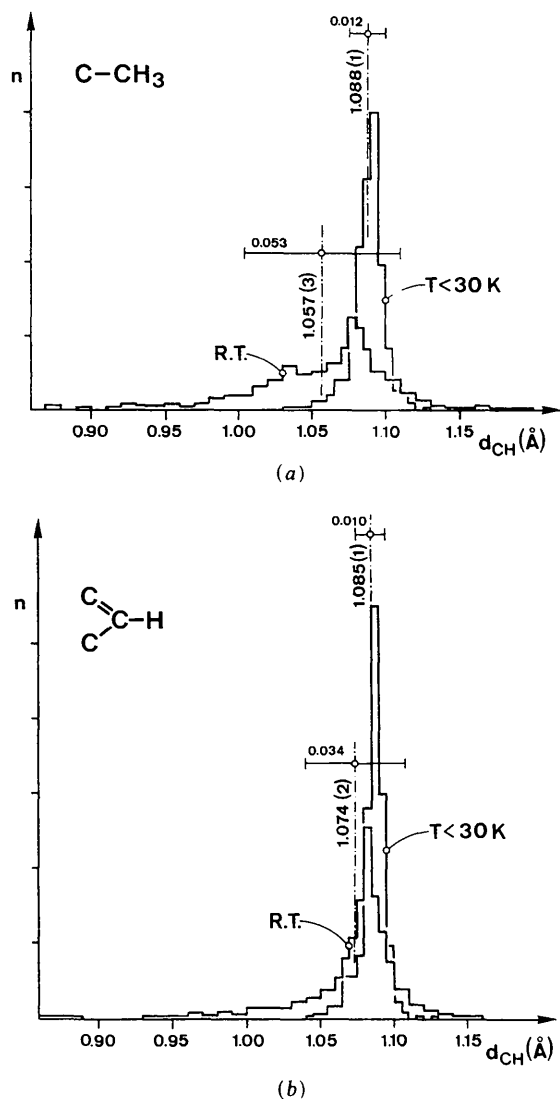
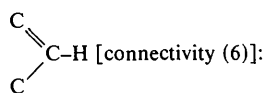


Fig. 1. Distribution of observed bond lengths d_{CH} at room temperature and at low temperatures, $T < 30$ K. (a) C-CH₃ [connectivity (1)]: the distributions peak between 1.075 and 1.080 Å at room temperature and between 1.090 and 1.095 Å at $T < 30$ K. (b)



the distributions peak between 1.080 and 1.085 Å at room temperature and between 1.085 and 1.090 Å at $T < 30$ K. The distributions are normalized in such a way that all curves cover the same area. For the room-temperature distributions, the same step width as for $T < 30$ K (0.005 Å) is used only in the peak regions.

In the distributions of Fig. 1, the peak positions are much less affected by thermal vibrations than the average values: for the methyl group, the maximum value (*i.e.* the most frequently observed d_{CH}) increases by only 0.015 Å upon cooling, whereas $\langle d_{\text{CH}} \rangle$ increases by 0.03 Å. For connectivity (6), the corresponding shifts are 0.005 and 0.011 Å, respectively. This implies that at room temperature relatively many C-H bonds show only a small reduction in bond length.

Temperature dependence of mean observed bond lengths

Only for connectivities (1) and (6) can the temperature dependence of the mean observed bond lengths be studied in greater detail. The temperatures $T \leq$ room temperature were divided into six ranges. A finer division unacceptably reduces the number of data per interval and hence the statistical quality. The organic neutron crystal structures determined at $T > 300$ K are far too few to be included.

For the six temperature ranges, the mean observed bond lengths and the corresponding r.m.s. deviations are listed in Table 3 and $\langle d_{\text{CH}} \rangle$ is plotted against $\langle T \rangle$, the mean temperature in the intervals in Fig. 3. For connectivity (6), we interpret the exceptionally short $\langle d_{\text{CH}} \rangle$ for $T < 15$ K as an outlier owing to the small number of data in that interval.

Fig. 3 illustrates that, for the methyl group, bond shortening by thermal vibrations reduces only slowly upon cooling and is still significant at liquid-nitrogen temperatures. Only for the last two temperature ranges, $15 \leq T < 30$ and $T < 15$ K, a difference of

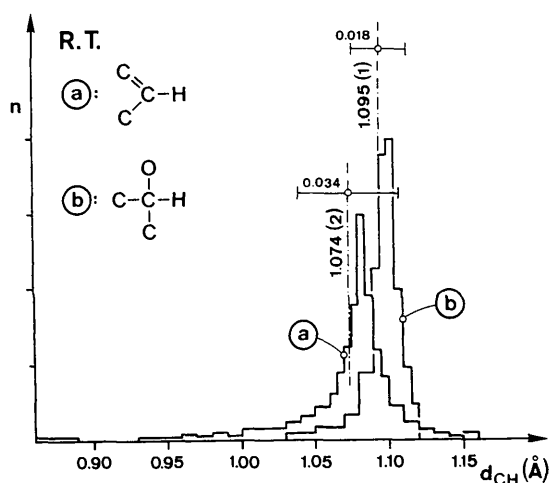
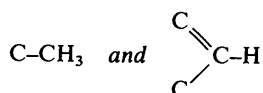


Fig. 2. Distribution of observed bond lengths d_{CH} at room temperature for connectivities (5) and (6). The distributions are normalized to cover the same area; they peak between 1.080 and 1.085 Å for connectivity (6) and between 1.100 and 1.105 Å for connectivity (5).

Table 3. Temperature dependence of mean observed C-H bond lengths $\langle d_{\text{CH}} \rangle$ (given in Å) in

$\langle T \rangle$: weighted mean temperature, $\langle T \rangle = \sum_i T_{\text{CH},i} / n_{\text{CH}}$, n_{struct} , n_{CH} , d_{CH} , r.m.s. dev. defined in Table 1.

T range (in K)	$\langle T \rangle$	n_{struct}	n_{CH}	$\langle d_{\text{CH}} \rangle$	R.m.s. dev.
C-CH₃					
Room temperature	RT	47	390	1.057 (3)	0.053
125 ≤ T < 295	259	5	45	1.070 (8)	0.054
80 ≤ T < 125	96	12	111	1.082 (2)	0.022
30 ≤ T < 80	45	3	69	1.083 (2)	0.020
15 ≤ T < 30	20	14	249	1.089 (1)	0.012
T < 15	6	5	63	1.087 (2)	0.017
Connectivity (6)					
Room temperature	RT	82	504	1.074 (2)	0.034
125 ≤ T < 295	200	8	39	1.083 (2)	0.013
80 ≤ T < 125	95	34	289	1.084 (1)	0.023
30 ≤ T < 80	46	7	40	1.086 (2)	0.010
15 ≤ T < 30	19	18	303	1.086 (1)	0.008
T < 15	7	5	42	1.078 (2)	0.015

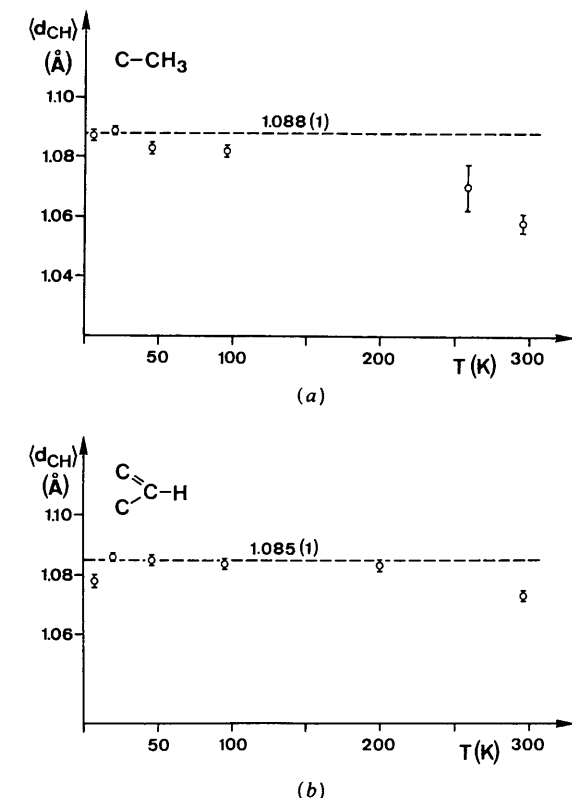
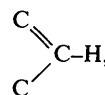


Fig. 3. Temperature dependence of mean observed C-H bond lengths $\langle d_{\text{CH}} \rangle$ for (a) C-CH₃ and (b) connectivity (6). Data are from Table 3. The dashed lines show the low-temperature mean value from Table 2.

$\langle d_{\text{CH}} \rangle$ cannot be observed within the limits of accuracy. For



bond shortening reduces faster upon cooling and at the temperatures of liquid nitrogen and liquid helium the average bond lengths differ by no more than the limits of accuracy, 0.001 to 0.002 Å; we associate this with the more rigidly confined orientation of the C-H bond compared with the methyl group.

Summary and discussion

This study is based on the neutron diffraction subset of the Cambridge Structural Database combined with three recent neutron crystal structures. The R value was limited to $R < 0.10$ and D atoms were excluded. The data were divided into certain connectivities of C-H and into the temperature ranges room temperature, $80 \leq T < 125$ and $T < 30$ K.

To ensure statistical relevance, connectivities were analysed only if at least 100 C-H bonds were available in at least five structures in at least one of the temperature ranges.

Connectivities given in Table 2 were not subdivided as this would significantly reduce the quantity of data in each group. This inevitably results in chemical heterogeneity. In general, the intra- and also the intermolecular environment of a specific C-H bond will influence d_{CH} . The distribution of observed d_{CH} is therefore not only determined by thermal vibrations and refinement accuracy but it also reflects effects due to covalent and noncovalent bonding.

At low temperatures ($T < 30$ K), the mean observed C-H bond lengths agree with the spectroscopic gas-phase values (Table 2).

At room temperature, the mean observed C-H bond lengths are shortened compared with the low-temperature values by ~ 0.03 Å for methyl groups, by almost 0.02 Å for methylene groups and by ~ 0.01 for the other connectivities (Table 2). Bond shortening becomes less pronounced the more rigidly the C-H orientations are stereochemically confined.

The individual d_{CH} show considerable scatter around the mean values ('r.m.s. dev.' in Table 2), reflecting the different vibration behaviour of H atoms in different crystal structures. This scatter reduces upon cooling and is most pronounced for the methyl group. The scatter is narrower the more rigidly the C-H orientations are confined.

The distributions of observed d_{CH} are asymmetric with the mean at lower values than the maximum (Fig. 1). This is extreme for the methyl group at room temperature, where the mean d_{CH} , 1.057 Å, is shorter by about 0.020 Å than the most frequently observed values, 1.075–1.080 Å. Furthermore, the peak posi-

tions are much less affected by differences in temperature than the average values. This implies that, at room temperature, a relatively large fraction of the observed bond lengths is only marginally influenced by thermal motions.

For the methyl group, bond shortening reduces only slowly upon cooling and is still significant at liquid-nitrogen temperatures. We associate this with the rotational freedom of the methyl group. For the other connectivities at $T \sim 100$ K, the observed bond lengths have already (or almost) reached the spectroscopically determined values (Fig. 3).

'True' chemical differences of C-H bond lengths in different connectivities are best studied at liquid-helium temperatures, but can also be observed at room temperature (Fig. 2). In general, the C-H bond length should increase with increasing (positive) partial charge on the C atom. This is actually observed in the present data set (Table 2), where the longest (d_{CH}) is found for connectivity (5).

This study was supported by the Bundesministerium für Forschung und Technologie, FKZ 03 SA3 FUB, and by the Fonds der Chemischen Industrie.

References

ALLEN, F. H. (1986). *Acta Cryst.* **B42**, 515-522.
ALLEN, F. H., BELLARD, S., BRICE, M. D., CARTWRIGHT, B. A.,

DOUBLEDAY, A., HIGGS, H., HUMMELINK, T., HUMMELINK-PETERS, B. G., KENNARD, O., MOTHERWELL, W. D. S., RODGERS, J. R. & WATSON, D. G. (1979). *Acta Cryst.* **B35**, 2331-2339.
BUSING, W. R. & LEVY, H. A. (1964). *Acta Cryst.* **17**, 142-146.
CALLOMAN, J. H., HIROTA, E., KUCHITSU, K., LAFFERTY, W. J., MAKI, A. G. & POTE, C. S. (1976). *Structure Data of Free Polyatomic Molecules. Landolt-Börnstein, Numerical Data and Functional Relationships in Science and Technology, New Series, Group II, Vol. 7.* Berlin: Springer Verlag.
CRAVEN, B. M. & SWAMINATHAN, S. (1984). *Trans. Am. Crystallogr. Assoc.* **23**, 71-81.
DUNITZ, J. D. & WHITE, D. N. J. (1973). *Acta Cryst.* **A29**, 93-94.
JEFFREY, G. A., RUBLE, J. R., MCMULLAN, R. K., DEFREES, D. J. & POPLE, J. A. (1981). *Acta Cryst.* **B37**, 1885-1890.
JOHNSON, C. K. & LEVY, H. A. (1974). *International Tables for X-ray Crystallography, Vol. IV*, pp. 311-336. Birmingham: Kynoch Press. (Present distributor Kluwer Academic Publishers, Dordrecht.)
KUHS, W. F. (1983). *Acta Cryst.* **A39**, 148-158.
SCHOMAKER, V. & TRUEBLOOD, K. N. (1968). *Acta Cryst.* **B24**, 63-76.
SRINIVASAN, R. & JAGANNATHAN, N. R. (1982). *Acta Cryst.* **B38**, 2093-2095.
STEINER, T., MASON, S. A. & SAENGER, W. (1990). *J. Am. Chem. Soc.* **112**, 6184-6190.
STEINER, T., MASON, S. A. & SAENGER, W. (1991). *J. Am. Chem. Soc.* **113**, 5676-5687.
STEINER, T. & SAENGER, W. (1992). *J. Am. Chem. Soc.* In the press.
WEBER, H.-P., CRAVEN, B. M. & MCMULLAN, R. K. (1983). *Acta Cryst.* **B39**, 360-366.
WEBER, H.-P., CRAVEN, B. M., SAWZIK, P. & MCMULLAN, R. K. (1991). *Acta Cryst.* **B47**, 116-127.

Acta Cryst. (1993). **A49**, 384-388

X-ray Diffraction when the Real Part of the Scattering Factor is Zero

BY TOMOE FUKAMACHI

Department of Electronic Engineering, Saitama Institute of Technology, Okabe, Saitama 369-02, Japan

AND TAKAAKI KAWAMURA

Department of Physics, Yamanashi University, Kofu, Yamanashi 400, Japan

(Received 13 February 1992; accepted 27 May 1992)

Abstract

A formulation of dynamical X-ray diffraction is given for use when studying X-ray diffraction intensities when the real part of the scattering factor is zero. Based on these formulae, the diffraction induced by the imaginary part of the scattering factor alone is studied for both the Bragg and Laue cases.

1. Introduction

Many studies using dynamical theories of X-ray diffraction (Zachariasen, 1945; James, 1963; Batter-

man & Cole, 1964; Miyake, 1969; Kato, 1974) have been carried out for absorbing crystals as well as for crystals without absorption. Some of the theories are not applicable to the case when the absorption is quite large or even the case when the real part of the scattering factor is zero. If we denote the normal scattering factor by f^0 , which depends on the reciprocal-lattice vector \mathbf{h} , and the real and the imaginary parts of the anomalous scattering factor by f' and f'' , respectively, f'' is usually assumed to be small compared with $f^0 + f'$. By taking the absorption effect as a perturbation, most of the experimental